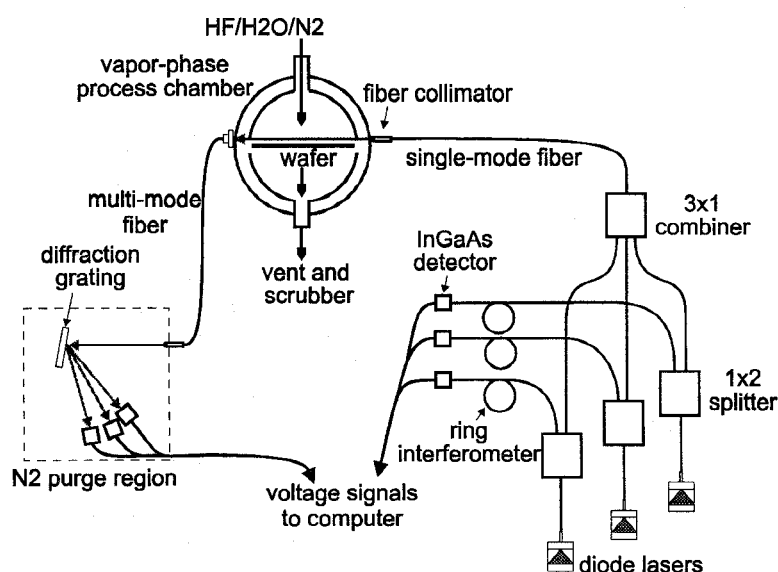
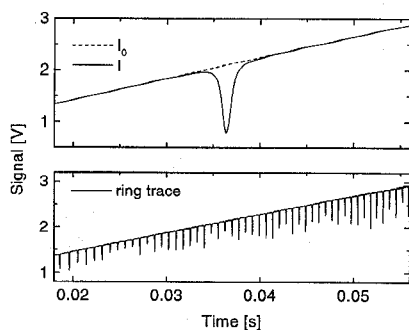


## Multiplexed Diode-Laser Sensor System...



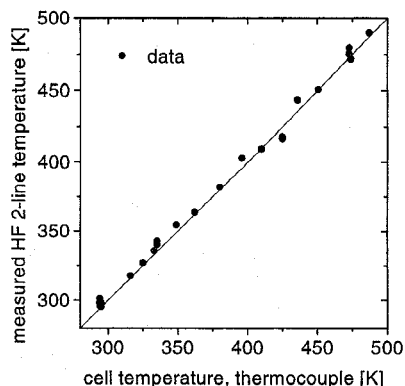
CTH15 Fig. 1. Schematic of a multiplexed diode-laser sensor system for vapor-phase process diagnostics.



CTH15 Fig. 2. Raw data traces of HF ( $P_3$  line,  $2\nu$  band) absorption recorded in a quartz reactor (296 K, 94.4 Torr, 20-cm path, 1.6% HF/ $N_2$  mixture).  $I_0$  is unabsorbed reference intensity.  $I$  is transmitted intensity through reactor. Free spectral range (FSR) of the ring interferometer is 840 MHz.

sensor system capable of *in situ* measurements of gas temperature and the concentrations of HF and  $H_2O$  to enhance process modeling and control.

The sensor system (Fig. 1) employs three narrow-linewidth ( $\sim 10$  MHz) distributed-feedback (DFB) tunable diode lasers operating at wavelengths near 1.31, 1.34, and 1.40  $\mu\text{m}$ . Particular transitions near these wavelengths were chosen for sensitive detection of HF ( $P_3$  and  $P_6$  transition in the  $2\nu$  band) and  $H_2O$  (ro-vibrational transitions in the  $\nu_1 + \nu_3$  and  $2\nu_1$  bands) concentrations and for thermometry. Each laser was maintained at a nearly constant temperature by a thermoelectric temperature controller (TEC). The injection current to each laser was ramp modulated at a 20-Hz rate to scan the wavelength across the selected transitions. Each laser output was coupled into a single-mode  $1 \times 2$  (10/90) optical fiber. The 90% output paths were combined (multiplexed) into a single path using a



CTH15 Fig. 3. Comparison of temperatures recorded in a quartz reactor using the two-line ratio method and thermocouples.

$3 \times 1$  beam combiner. The corresponding 10% output paths were directed through a ring interferometer to monitor the laser wavelength changes. The multiplexed beam was collimated with an aspheric lens and directed through the process chamber. The transmitted laser beam was focused into a multimode fiber and demultiplexed into the individual wavelength components by directing the beam onto a diffraction grating. Three InGaAs amplified photodetectors (200-kHz bandwidth) were used to measure the transmitted laser intensities at the three wavelengths. The voltage signals were sent to a data acquisition board mounted in a personal computer for analysis.

Figure 2 illustrates the transmission traces recorded by tuning a laser across the absorption transitions of HF (near 1312 nm) in a quartz reactor filled with 94.4 Torr of HF at 296 K. The top trace shows the transmission trace recorded through the reactor. The bottom trace shows the transmission trace through the ring interferometer and illustrates

the frequency tuning of the laser. The ratio of absorbances recorded by probing two HF transitions originating from different lower-energy states was used to infer the gas (Boltzmann) temperature. The technique was applied to record temperature measurements in HF/ $N_2$  mixtures over a wide range of conditions. The measurements were compared to thermocouple measurements (Fig. 3). The excellent agreement between the two methods validates the two-line technique and demonstrates the measurement accuracy ( $< 1\%$ ). Additional measurements of gas temperature, HF, and  $H_2O$  concentrations in an industrial-scale reactor are presented.

The system may be applied to record measurements of gas parameters during the cleaning process and provide important data to help determine the chemical mechanisms responsible in vapor-phase processes.

CTH16

11:45 am

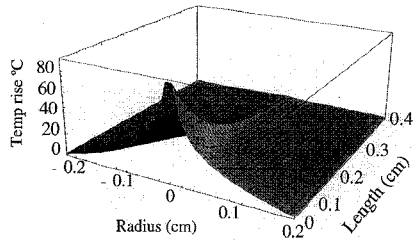
### Direct measurement of thermal lensing in $Cr^{3+}$ -doped colquirrites

Jason M. Eichenholz, Martin Richardson, Center for Research and Education in Optics and Lasers, University of Central Florida, 4000 Central Florida Blvd., Orlando, Florida 32816-2700; E-mail: jason@creol.ucf.edu

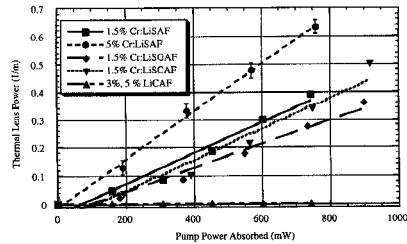
Longitudinal diode pumping of a solid-state laser material has the advantage of highly efficient fundamental mode operation.<sup>1</sup> The pump power is focused directly into the center of the laser rod and is absorbed predominantly in the  $TEM_{00}$  laser mode volume. This approach, however, gives rise to a large thermal gradient. The thermal gradient is the result of the strongly inhomogeneous thermal power density that heats the center of the crystal while the edges of the rod remain cool. This heating leads to stress, birefringence, surface elongation, refractive-index variation, thermal lensing, and ultimately mechanical fracture.<sup>2</sup> The measurement and compensation of these induced thermal effects in new solid-state media are therefore crucial to the scaling of new laser systems to higher powers.

We have utilized the results of previous studies<sup>1-3</sup> in the development of a two-dimensional code that takes into account the quantum defect, upconversion, and thermal quenching of fluorescence. This code provides the spatial distribution of temperature, upper-state lifetimes, and heating sources within a laser rod under longitudinal pumping, for all the colquirite laser materials. The output of this code for a 4-mm-diameter, 1.5% Cr:LiSGAF rod is shown in Fig. 1 for 1 W of pump power.

Thermal lensing has not yet been considered in end-pumped colquirite laser systems. Three different mechanisms—thermally induced index of refraction gradients, stress-induced index of refraction gradients, and the curvature of the rod ends—each contribute to thermal lensing in the colquirites. We have measured the thermally induced lensing in colquirite laser crystals, using a pump-probe technique.<sup>4</sup> By determining the change in divergence of the probe beam, the thermally induced focal length can be calculated.



**CTH16** Fig. 1. Temperature rise in a 1.5% Cr:LiSGAF laser rod as a function of radius and length for an incident pump power of 1 W.



**CTH16** Fig. 2. Experimental data showing thermal lensing focal power versus absorbed pump power.

The measured thermally induced focal power ( $1/f_{th}$ ) of the colquirite laser samples is shown in Fig. 2. The induced focal power for 1.5 and 5% Cr:LiSAF, 1.5% Cr:LiSGAF, 3% Cr:LiSCAF, and 3 and 5% Cr:LiCAF is plotted as a function of absorbed pump power. Figure 2 also shows that the thermal focal length is nearly inversely proportional to the absorbed pump power, which is in good agreement with thermal lensing theory.<sup>5</sup> We were unable to measure any thermally induced lensing in Cr:LiCAF. The strongest thermally induced focal length in these experiments was  $>1.5$  m long.

The temperature-dependent refractive index ( $dn/dT$ ) in LiCAF and LiSAF has been quantitatively measured to be negative. However, because the stresses are nearly always positive, the linear combination of the temperature- and stress-induced refractive-index changes tend to cancel, resulting in our measurement of reduced positive thermal lensing.

1. A.K. Cousins, IEEE J. Quantum Electron. **28**, 1057–1069 (1992).
2. M. Ohmi, K. Naito, K. Ishikawa, M. Akatsuku, T. Sato, M. Yamanaka, S. Nakai, Jpn. J. Appl. Phys. **33**, 2579–2585 (1994).
3. F. Balembois, F. Falcoz, F. Kerboull, F. Druon, P. Georges, A. Brun, IEEE J. Quantum. Election. **33**, 269–277 (1997).
4. D.C. Burnham, Appl. Opt. **9**, 1727–1728 (1970).
5. W. Koehner, *Solid State Laser Engineering*, 4th ed. (Springer-Verlag, New York 1996).

**CTHJ** 10:30 am–12:30 pm  
Room 102

**Ultrashort Pulse Generation**

Jeffrey A. Squier, *University of California, San Diego, President*

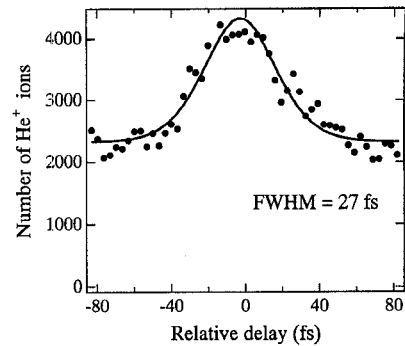
**CTHJ1 (Invited)** 10:30 am

**Ultrashort pulse generation by high-order harmonics**

S. Watanabe, Y. Kobayashi, T. Sekikawa, Y. Nabekawa, *Institute for Solid State Physics, University of Tokyo, 7-22-1 Roppongi, Minato-ku, Tokyo 106, Japan*

Remarkable progress has recently been made in the generation of ultrashort pulses. Pulses  $<5$  fs have been demonstrated at 800 nm.<sup>1,2</sup> These pulses contained only two or three optical cycles and are thus approaching the ultimate limit. For further pulse shortening, a shorter wavelength is obviously desirable. High-order harmonics are promising candidates for this purpose. The bandwidth of high-order harmonics is much broader than that of the fundamental pulse. The problem, however, is how to measure the pulse width. Pulse widths of high-order harmonics were measured in the range of 100 fs by cross correlation with the fundamental pulse, but it is difficult to measure the width of pulses much shorter than the fundamental pulse. We demonstrated for the first time the autocorrelation measurement in the extreme ultraviolet region by using the two-photon ionization of rare gases and observed 27-fs pulses at the 9th Ti:sapphires harmonic of (TiS) laser.

The experimental setup for the autocorrelation measurement is shown in Fig. 1. In this experiment, a 22-fs, 22-TW TiS laser system with a repetition rate of 10 Hz was operated at 1 TW level with 34-fs pulses.<sup>3</sup> The fundamental pulses were spatially divided into two beams in a delay line before a pulse compressor. The spatially separated beams were focused by a spherical mirror with a 1-m radius of curvature. The 1-mm-thick Xe gas envelope with 800- $\mu$ m holes on both sides was placed 15 mm before the focal point. In this configuration, the pulse energy of the 9th harmonic was increased up to 50 nJ with an input energy of

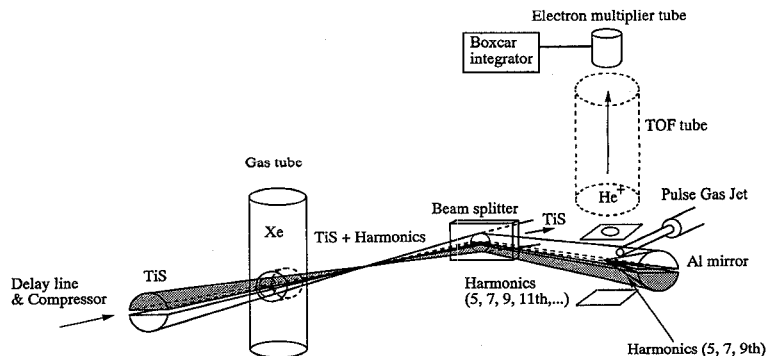


**CTHJ1** Fig. 2. Autocorrelation trace of the 9th harmonic by two-photon ionization of He. Experimental points are fitted to a  $\text{sech}^2$  pulse shape, giving a 27-fs pulse width.

44 mJ. A beam splitter and an Al-coated mirror were used to eliminate the fundamental pulse and the harmonics above the 11th that can ionize rare gases by one-photon absorption. The beam splitter reflects  $\sim 40\%$  of harmonics above the 7th and passes 99.2% of the fundamental beam, 96% of the 3rd harmonic, and some of the 5th harmonic. The reflected harmonics were focused in a time-of-flight analyzer by an  $f = 10$ -cm concave mirror. A pulse gas jet was placed in the focal point to supply rare gases for ionization. The ionization signal due to He was confirmed to be mainly due to the 9th harmonic by measuring the dependence of the ionization signal on the intensity of the individual harmonic.

Figure 2 shows the autocorrelation trace of the 9th harmonic by the two-photon ionization of He. The fitting to a  $\text{sech}^2$  pulse shape gives a pulse width of 27 fs. This value is 20% less than the fundamental pulse width ( $\tau$ ),  $34 \pm 5$  fs, but is much greater than 11 fs estimated from  $\tau\sqrt{q}$  ( $q = 9$ ) and 6 fs estimated from the Fourier transform. Possible reasons for this large difference are the saturation of harmonic yields against the laser intensity and the intensity-dependent phase of the atomic dipole. The calculation of intensity- and space-dependent harmonic yields predicts the generation of 8 fs at the optimum intensity. In the next experiment, we will attempt to get the shorter pulse width by using a kHz TiS laser with pulse duration  $<20$  fs.

1. A. Baltuska, Z. Wei, M.S. Pshenichnikov, D.A. Wiersma, Opt. Lett. **22**, 102 (1997).



**CTHJ1** Fig. 1. Experimental setup for the autocorrelation measurement.